Mechanical exfoliation of indium tin oxide as saturable absorber for Q-switched Ytterbium-doped and Erbium-doped fiber lasers

B. Nizamani [a], A.A.A. Jafry [b], Sameer Salam [a,c], Mustafa Mohammed Najm [a], M.I.M. Abdul Khudus [d], E. Hanafi [a], S.W. Harun [a,*]

[a] Photonics Engineering Laboratory, Department of Electrical Engineering, University of Malaya, 50603 Kuala Lumpur, Malaysia
[b] Department of Physics, Faculty of Science, Universiti Teknologi Malaysia, 81310 Skudai, Johor, Malaysia
[c] Faculty of Information Technology, Imam Ja'afar Al-Sadiq University, Baghdad, Iraq
[d] Department of Physics, Faculty of Science, University of Malaya, 50603 Kuala Lumpur, Malaysia

ABSTRACT

This work reports mechanically exfoliated indium tin oxide (ITO) as saturable absorber (SA) for Q-switched operation in fiber lasers. The ITO is mechanically exfoliated from 99.99% pure In_2O_3/SnO_2. As ITO has a broad operational wavelength from visible to infrared, indium tin oxide saturable absorber (ITO-SA) is incorporated into ytterbium-doped fiber laser (YDFL) and erbium-doped fiber laser (EDFL) cavity for Q-switched operation. The Q-switched spectrum was observed to be centered at 1038.25 nm for ytterbium-doped fiber and 1557.8 nm for erbium doped fiber. The ITO-SA has a linear absorption of 2.25 dB and 2.5 dB at 1 μm and 1.5 μm respectively. A narrow pulse width was observed in the EDFL operating at 0.95 μs. For the first time, ITO-SA is incorporated to YDFL cavity.

1. Introduction

Reliable and scalable pulsed lasers are increasing in demand for various applications including telecommunication, laser engraving, material processing and medical treatments [1–5]. In contrast to continuous-wave (CW), pulsed laser is preferred as it gives high output power and pulse energy. Pulsed laser can be achieved either by passive or active means. Active means of generating pulsed lasers typically includes some elements such as lenses, mirrors or modulators, which requires external signals and can thus increase the complexity of the laser system and may degrade the performance with time [6]. Pulsed laser operation may also be achieved via passive methods such as by the insertion of a saturable absorber (SA) in the fiber laser cavity either by deposition on a side-decladded, D-shape fiber inserted to the cavity or via direct insertion by sandwiching it between fiber ferrules [7,8].

Semiconductor saturable absorber mirrors (SESAMs) is first studied as a SA that gives a stable pulse laser operation [9]. Due to the high cost and fabrication complexities of SESAMs, many other materials are developed and incorporated as a SA in the fiber laser cavity, including carbon nanotubes (CNTs), graphene, transition-metal dichalcogenides (TMDs), topological insulators (TIs) and black phosphorus (BP) [10–15]. For the past few years, CNTs and graphene has been widely employed as SAs. CNTs offer a low-cost solution, but the wavelength operation depends on the nanotube diameter. Graphene allows stable and flexible pulsed laser operation and has thus been widely used as a

pulse initiators in near-infrared (NIR) laser cavities [16,17]. However, the low modulation depth of Graphene encouraged researchers to develop new materials as a SA for the fiber laser cavity. Since the introduction of Graphene, other materials were incorporated inside a fiber laser cavity which have reveal exceptional saturable absorption properties that have contributed to vast research efforts in short-pulsed laser generation.

Indium tin oxide (ITO) is widely employed as a transparent conductive oxide (TCO) due to its optical transparency and electrical conductivity. ITO is often used in flat panel displays such as liquid crystal displays (LCD); solar cells and organic light emitting devices (OLED) [18–20]. For O-LED, ITO has low electrical resistivity of 2×10^{-4} Ω cm and high transmission of about 92% in visible and near-infrared spectrum [21,22]. Alam et al. have recently reported ITO having large optical nonlinearity and ultrafast recovery time of 360 fs [23]. ITO also has a broad operational wavelength from the visible to near-infrared region. As a result, its operational regime for all fiber lasers can be stretched from 1 μm to 2 μm wavelength spectrum or beyond it. Recently, Guo et al. [24] have reported the study of ITO as SA for erbium-doped fiber laser (EDFL) generating Q-switched pulses at the operating spectrum of 1.5 μm region. The pulse width and repetition rate were reported to be 1.15 μs and 81.28 kHz, respectively. Their method involving a co-precipitation of ITO nanocrystals onto the fiber-ferrule introduced impurity to the SA device. As the liquid
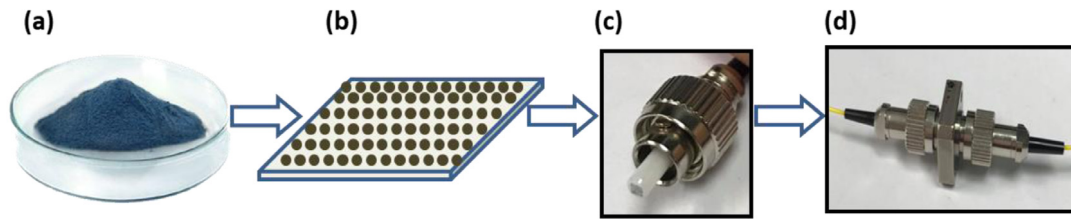

Fig. 1. Fabrication of ITO-SA (a) ITO source material (b) ITO over scotch tape (c) ITO-SA over fiber ferrule (d) ITO-SA inserted in cavity via fiber adaptor.

ITO was exposed to the external environment, making it vulnerable to oxidation and other chemical reactions. Here, we provide a straightforward and simple mechanical exfoliation to synthesis ITO-based SA. The improvement of Q-switched pulses was achieved with a much higher repetition rate of 103 kHz and a narrower pulse width of 0.95 μs. Our results are comparable to the studies on 2-dimensional (2D) materials as SA, such as bismuth selenide (Bi_2Se_3), which was reported to emit Q-switched with the maximum repetition rate and minimum pulse width of 40.1 kHz and 4.9 μs, respectively [25]. Recently, Luo et al. have demonstrated a molybdenum disulfide (MoS_2) as a Q-switcher for both EDFL and ytterbium-doped fiber laser (YDFL) [26]. However, the minimum pulse width remained wider at 7.5 μs for EDFL and 5.8 μs for YDFL. In this work, we improved the Q-switching performance in both 1 and 1.5 μm region, by obtaining a minimum pulse width of 1.8 μs and 0.95 μs, respectively. For the first time, ITO as SA was demonstrated as SA in the YDFL cavity, and mechanical exfoliation of ITO was introduced in the EDFL cavity.

2. Preparation and characterization

Indium tin oxide saturable absorber (ITO-SA) was prepared by mechanical exfoliation as it is a simple and reliable process formerly used for materials such as TI, graphene and BP [17,27,28]. As shown in Fig. 1(a), the ITO was mechanically extracted from a 99.99% pure In_2O_3/S_nO_2 (Materion Advanced Materials Technologies and services, Taiwan) of 90:10 wt %. The ITO particles were exfoliated by using scotch tape as depicted in schematic diagram of Fig. 1(b). The scotch tape was folded and pressed persistently to form evenly distributed ITO thin film over it. A fiber ferrule was then cleaned with isopropyl alcohol and a small portion of ITO-SA over scotch tape was then cut and placed over fiber ferrule as shown in Fig. 1(c). The ITO-SA was then slot in between two fiber ferrules of EDFL and ytterbium-doped fiber laser (YDFL) cavity setup via FC/PC adapter (FCPC-FCPC-D100) as shown in Fig. 1(d). Fiber connectors introduced insertion loss of ~0.5 dB.

The presence of indium, tin and oxygen was verified by energy dispersive X-ray spectroscopy (EDS) as illustrated in Fig. 2(a). Intensity peaks at desired energy levels ensured the presence of elements at atomic percentage quantified as In (41 at.%), Sn (39 at. %), O (20 at. %) with an marginal error of ±2%. Fig. 2(b) shows a morphological structure of exfoliated ITO under the field emission scanning electron microscopy (FESEM). The ITO particles varied in size, with an average of 150 nm. The linear absorption of ITO-SA is shown in Fig. 2(c), where it can be observed that there was nearly a flat linear absorption in the wavelength region of 950 nm to 1600 nm. The ITO-SA gave linear absorption of 2.25 dB at 1 μm and 2.5 dB at 1.5 μm for the Ytterbium-doped fiber laser (YDFL) and EDFL operation, respectively. The nonlinear absorption property of ITO-SA was analyzed using the balanced twin-detector technique. A 1557.7 nm mode-locked source with a pulse width of 3.6 ps and a repetition rate of 1.8 MHz was used as a laser source. The light was amplified with an erbium-doped fiber amplifier (EDFA) before being connected to the optical attenuator. Finally, 50% of outgoing radiation passes through the SA device via a 3-dB coupler, with the remainder propagating through a bare single-mode fiber (SMF-28). The measurement shows a saturable absorption

(α_s) of 1%, a non-saturable absorption (α_{ns}) of 68.4%, and a saturable intensity of 6.39 MW/cm^2, as depicted in Fig. 2(d). At 1050 nm, the saturable absorption was obtained at about 0.8%.

3. Experimental setup

Fig. 3 illustrates the experimental setup of fiber laser cavity. Fig. 3(a) shows YDFL cavity setup, a 980 nm laser diode (LD) pump is employed as input power source for YDFL. The cavity is pumped via the 980 nm port of the wavelength division multiplexer (WDM) by a 980 nm LD pump. A single mode ytterbium-doped fiber (YDF) of 1.5 m length is connected after the WDM as a gain medium. The YDF has core diameter of 4 μm and numerical aperture of 0.20. A polarization independent isolator (PI-ISO) is then connected with the setup to ensure unidirectional propagation of signal inside the YDFL cavity. The ITO-SA was then inserted into the cavity after PI-ISO by using fiber connectors. After the ITO-SA, an 80:20 coupler is connected where the 80% signal port is connected back to WDM 1064 nm port as feedback and the other 20% signal port is connected to the outputs of YDFL. Total length of YDFL cavity is measured to be approximately 10 m. Fig. 3(b) illustrates the schematic diagram of proposed EDFL cavity setup. A 980 nm LD pump is connected to the EDFL setup via 980 nm port of 980/1550 nm WDM. A 2 m long erbium-doped fiber (EDF) is connected to the WDM as a gain medium. EDF has numerical aperture, core diameter, group velocity dispersion (GVD) and absorption coefficient of 0.16, 4 μm, 27.6 ps^2/km, and 23 dB/m respectively. A PI-ISO is included in the setup to avoid back reflection of light. The ITO-SA is then inserted to the EDFL setup which is connected to a 50:50 coupler. 50% output of coupler is connected with 1550 nm port of WDM for the signal to oscillate inside cavity while the other 50% output of coupler is connected to see the output results. The cavity length is approximately 6 m including all the standard single mode fiber (SMF-28) used. The outputs of both YDFL and EDFL are analyzed by optical power meter (OPM) (Thorlabs:PM100D) for output power; optical spectrum analyser (OSA) (Yokogawa:AQ6370B) for the wavelength spectrum; 7.8 GHz radio frequency spectrum analyser (RFSA) to see the frequency spectrum of pulsed laser; and 350 MHz oscilloscope (GWINSTEK:GDS-3352) to observe the pulse train. The oscilloscope and RFSA are connected via fast photo detector (Thorlabs: DET10D/M) to investigate the output in the optical domain.

4. Results and discussion

Q-switched operation of the YDFL is shown in Fig. 4. YDFL cavity worked in continuous-wave (CW) operation at 94 mW, while Q-switched pulses appeared at pump powers of 180 mW to 216 mW after insertion of ITO-SA to the cavity. At the pump power of 216 mW, a CW operation centered at wavelength peak of 1037 nm was observed as shown in Fig. 4(a). At the pump power of 216 mW, the center wavelength shifted slightly to 1038.25 nm in pulsed operation, as shown in Fig. 4(b). Fig. 4(c) shows pulse train of Q-switched operation at pump power of 216 mW. The pulse width was observed to be 1.8 μs, while peak to peak distance between two pulses was measured to be 13 μs.

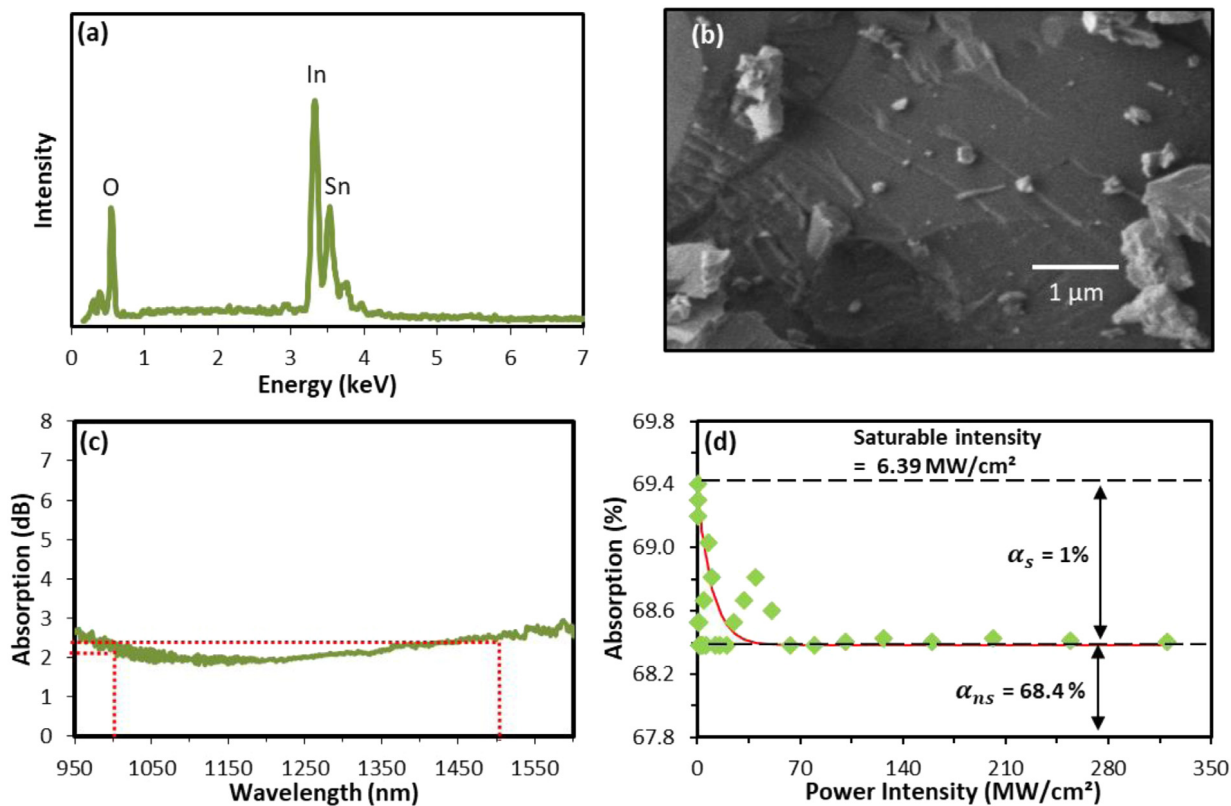**Fig. 2.** (a) EDS spectrum (b) FESEM image (c) Linear absorption of ITO-SA (d) Non-linear absorption of ITO-SA.
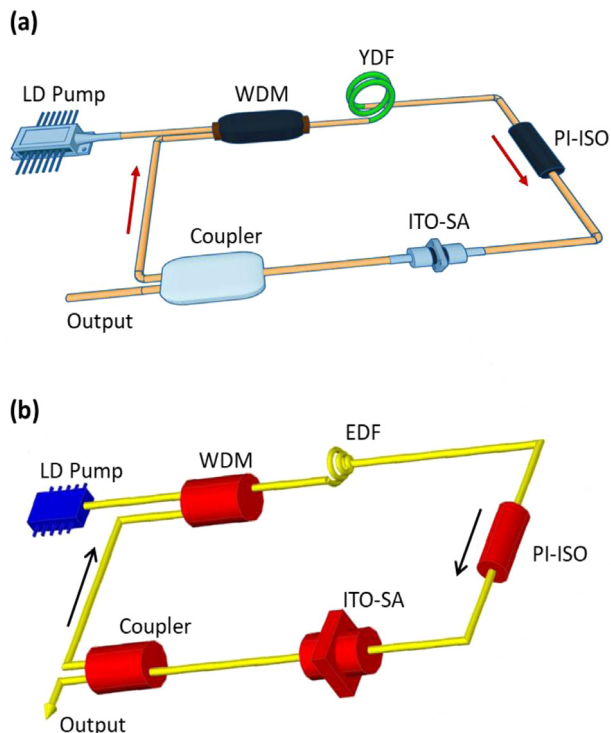

Fig. 3. Fiber laser setup (a) Ytterbium-doped fiber laser (b) Erbium-doped fiber laser.

Smooth and symmetric pulses were observed at the oscilloscope with no obvious fluctuations in pulse amplitude or pulse shape, indicating that the Q-switched operation was stable. Fig. 4(d) gives frequency spectrum of Q-switched YDFL having fundamental frequency of 78 kHz, with signal-to-noise ratio (SNR) of 55 dB, at a pump power of 216 mW. Several frequency peaks observed in frequency spectrum at span of 800 kHz ensure stable Q-switched operation. The maximum pulse energy was recorded to be 4.55 nJ, increasing linearly from 2.85 nJ to 4.55 nJ with pump power of between 180 mW to 216 mW as shown in Fig. 4(e). The repetition rate increased from 55.4 kHz to 78 kHz, while the pulse width decreased from 3.2 μs to 1.8 μs with the increase of pump power. The increase in the repetition rate and decrease of pulse width with increased pump power is consistent with Q-switched operation of our YDFL as shown in Fig. 4(f). Q switching operation of the YDFL is only possible within a small input power range, attributed to the high threshold pump power of Q-switched. By reducing the saturable intensity of the SA device and optimizing the YDFL cavity, the power range of Q-switched can be increased, allowing the Q-switch operation at a lower threshold pump. By increasing the pump power from 216 to 270 mW, we observed the disappearance of the Q-switched pulse. Later, we bring the LD pump back to 216 mW, and the same temporal pulse performance recovered. Thus, the SA device has an optical damage threshold which is higher than 270 mW. To the best of our knowledge, this is the first time ITO is reported as a SA operating in YDFL.

Fig. 5 shows the Q-switched operation of an EDFL. CW operation of EDFL was observed at pump power of 30 mW before inserting ITO-SA to the setup. Q-switched operation was achieved after insertion of the ITO-SA at the pump power range of 35.2 mW to 188 mW. At the pump power of 188 mW, the center wavelength peak shifted from 1562.3 nm of CW operation (before insertion of ITO-SA) to 1557.8 nm of Q-switched operation (after insertion of ITO-SA). The shift in wavelength
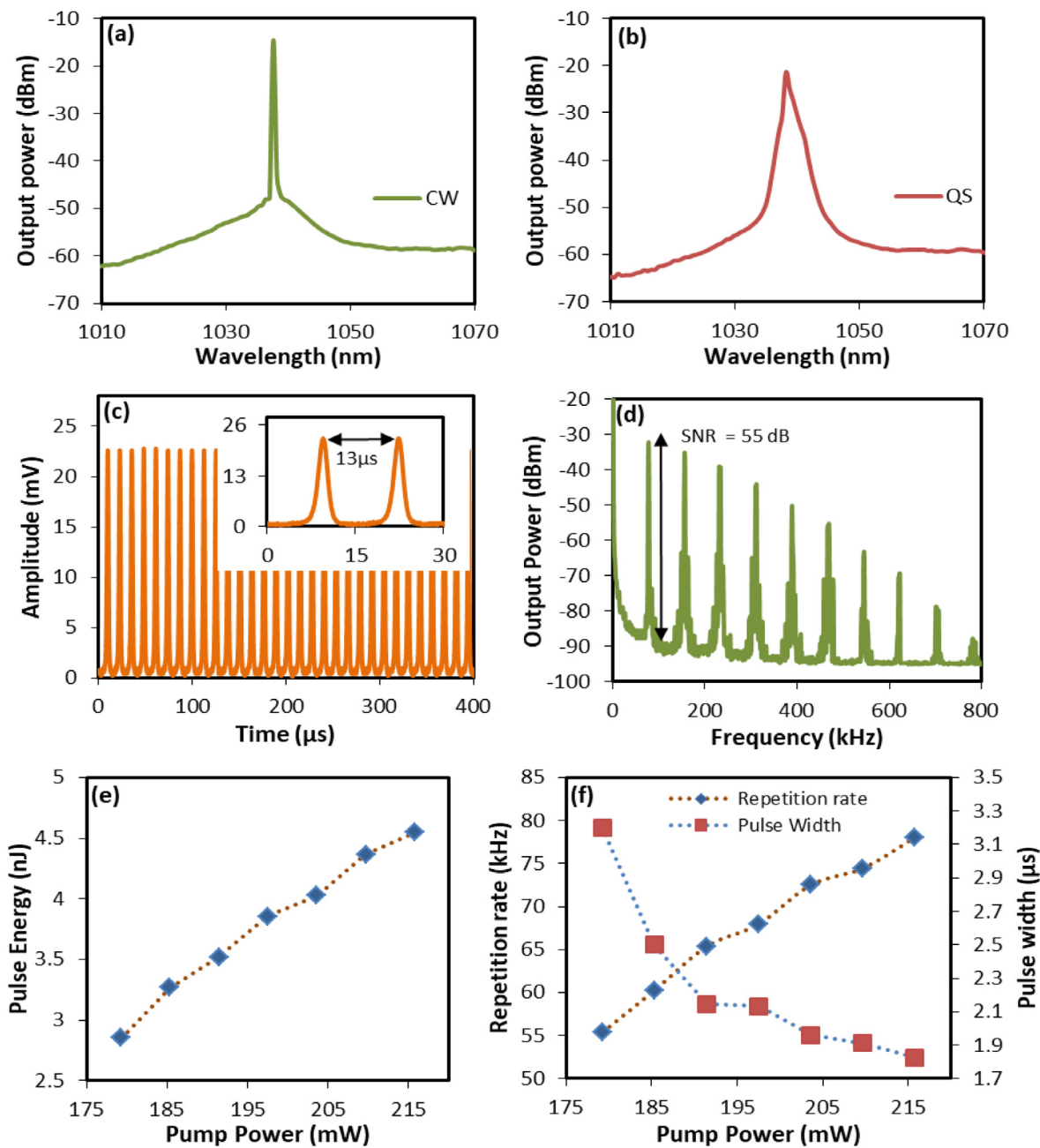
Fig. 4. YDFL operation (a) Continuous wave at 216 mW pump power (b) Q-switched pulse at 216 mW pump power (c) Pulse train (d) Frequency spectrum (e) Pulse energy graph (f) Repetition rate and pulse width plot.

peak was observed over the OSA in wavelength span of 1545 nm to 1575 nm as shown in Fig. 5(a). The frequency spectrum observed at 188 mW pump power is shown in Fig. 5(b), where an SNR of 59 dB at repetition rate of 103 kHz and more than 15 frequency peaks were observed in 1800 kHz span of RFSA. From Fig. 5(c) where the Q-switched pulse laser was operating at 188 mW the repetition rate was observed to be 103 kHz and a narrow pulse width of 0.95 μs was achieved. The peak to peak distance between two pulses was measured to be 9.6 μs. A clear view of two pulses in Fig. 5(c) shows the pulses retained their symmetric shape and the pulse amplitude showed no obvious fluctuation giving that the pulses were stable.

The output power and pulse energy of Q-switched EDFL are plotted with pump power in Fig. 6(a). The output power and pulse energy were observed to increase with the increase of pump power from 35.2 mW to 188 mW. The maximum output power achieved was approximately 1.47 mW while pulse energy was achieved to be 14.26 nJ. In Fig. 6(b) we have plotted Q-switched operation of EDFL at pump power between 35.2 mW to 188 mW, repetition rate increased from 54.8 kHz to 103 kHz and pulse width decreased from 3.43 μs to 0.95 μs. Q-switched operation of EDFL is the enhancement of our previous work, which reported ITO-SA by coating ITO over a D-shape fiber [29]. The work used a 13.6 m EDFL cavity, in contrast, we shorten the cavity length to 6 m in this work. As a result, a pulse performance with a higher repetition
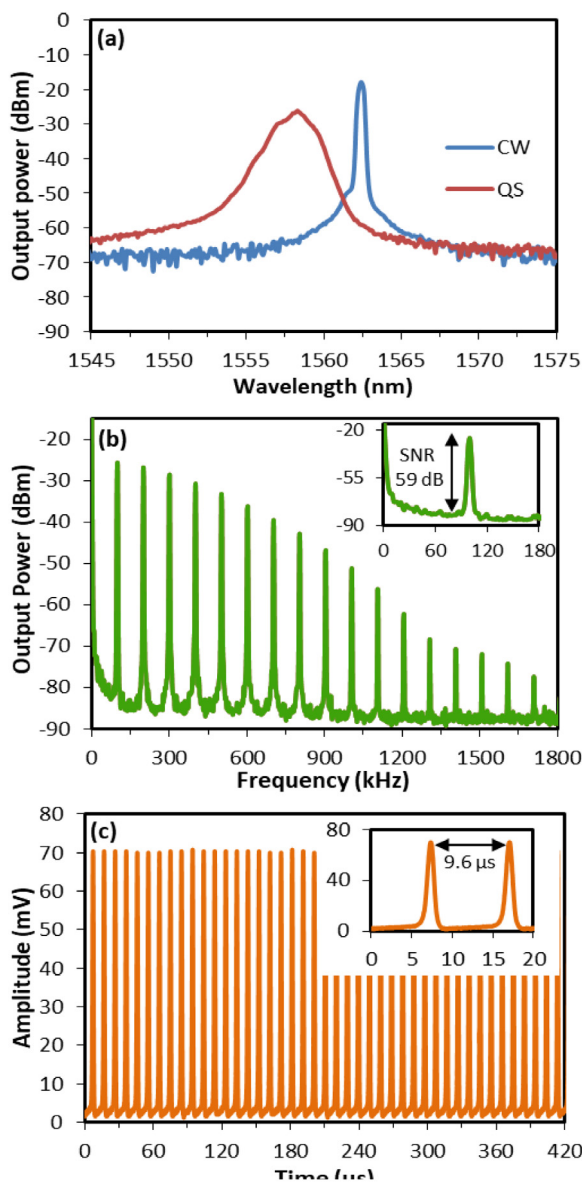
Fig. 5. EDFL operation at 188 mW (a) Center wavelength operation of CW and Q-switched pulse (b) Output frequency spectrum (c) Pulse train.
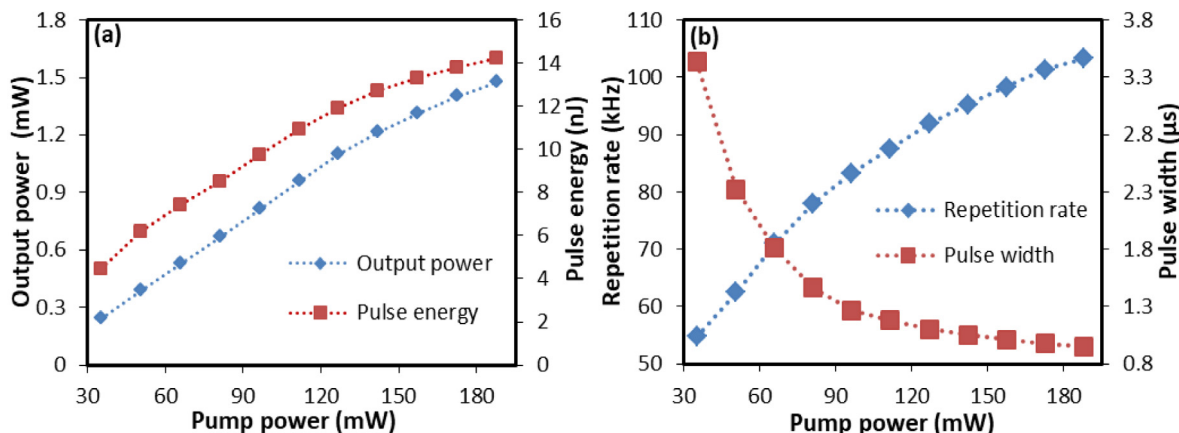
rate and a narrower pulse width was obtained as the pulse travels in a shorter time with a decrease in the cavity length [30]. A significant improvement in output power and pulse energy was also realized, this is due to the implementation of an optical coupler with a higher output ratio (50%) compared to 10% previously. The mechanical exfoliation provides a good alternative for the SA implementation method in an all-fiberized laser cavity, as proven by its excellent Q-switched performance, which is comparable to the ITO deposited onto D-shaped fiber. This work suggests a simple technique with an outstanding pulsed performance compared to complicated sample preparation of D-shaped fiber-based SA.

There is no mode-locking operation observed even if we tuned the LD pump towards the maximum values (200 mW for EDFL and 270 mW for YDFL). This may be due to the large splice losses inside the laser cavity, which suppressed the number of oscillating longitudinal modes, hence preventing mode-locking operation. However, by constructing the ring cavity with optimum length and low-loss, the mode-locking operation may be realized [31]. Furthermore, the extension of cavity length might introduce mode-locking operation, as it enables a balance between dispersion and nonlinearity inside the laser cavity.

5. Conclusion

As ITO has a broad wavelength operation, we developed Q-switched YDFL and EDFL which operate at center wavelengths of 1038.25 nm and 1557.8 nm. A novel study with Q-switched YDFL operation of ITO-SA is reported in this work. Here, the ITO-SA was simply prepared by mechanical exfoliation without any chemical procedures. The preparation of ITO-SA was done by a cost-effective method that did not involve any expensive devices such as a sputtering chamber. A short pulse width of 0.95 μs and high pulse energy of about 14.26 nJ was achieved with EDFL. While pulse width and pulse energy in YDFL operation varied from 3.2 μs to 1.8 μs and 2.85 nJ to 4.55 nJ respectively. ITO-SA proves to be a suitable SA which can operate in a wider wavelength regime.

Declaration of competing interest

The authors declare that they have no known competing financial interests or personal relationships that could have appeared to influence the work reported in this paper.

Fig. 6. Q-switched EDFL operation (a) Pulse energy and output power with pump power (b) Repetition rate and pulse width with pump power.

References

[1] H.M. Oubei, et al., 4.8 Gbit/s 16-QAM-OFDM transmission based on compact 450-nm laser for underwater wireless optical communication, Opt. Express 23 (18) (2015) 23302–23309.

[2] M.J. O'Mahony, et al., The application of optical packet switching in future communication networks, IEEE Commun. Mag. 39 (3) (2001) 128–135.

[3] R. Lahoz, et al., Laser engraving of ceramic tiles, Int. J. Appl. Ceram. Technol. 8 (5) (2011) 1208–1217.

[4] D.S. Correa, et al., Femtosecond laser in polymeric materials: microfabrication of doped structures and micromachining, IEEE J. Sel. Top. Quantum Electron. 18 (1) (2011) 176–186.

[5] S. Shah, T.S. Alster, Laser treatment of dark skin, Am. J. Clin. Dermatol. 11 (6) (2010) 389–397.

[6] M. Delgado-Pinar, et al., Q-switching of an all-fiber laser by acousto-optic modulation of a fiber Bragg grating, Opt. Express 14 (3) (2006) 1106–1112.

[7] B. Nizamani, et al., Mode-locked erbium-doped fiber laser via evanescent field interaction with indium tin oxide, Opt. Fiber Technol., Mater. Devices Syst. 55 (2020) 102124.

[8] S. Salam, et al., Soliton mode-locked Er-doped fiber laser by using Alq3 saturable absorber, Opt. Laser Technol. 123 (2020) 105893.

[9] U. Keller, et al., Semiconductor saturable absorber mirrors (SESAM's) for femtosecond to nanosecond pulse generation in solid-state lasers, IEEE J. Sel. Top. Quantum Electron. 2 (3) (1996) 435–453.

[10] D.-P. Zhou, et al., Tunable passively Q-switched erbium-doped fiber laser with carbon nanotubes as a saturable absorber, IEEE Photonics Technol. Lett. 22 (1) (2009) 9–11.

[11] G. Sobon, et al., Linearly polarized, Q-switched Er-doped fiber laser based on reduced graphene oxide saturable absorber, Appl. Phys. Lett. 101 (24) (2012) 241106.

[12] H. Ahmad, et al., Passively Q-switched erbium-doped fiber laser at C-band region based on WS 2 saturable absorber, Appl. Opt. 55 (5) (2016) 1001–1005.

[13] H. Zhang, et al., Molybdenum disulfide (MoS 2) as a broadband saturable absorber for ultra-fast photonics, Opt. Express 22 (6) (2014) 7249–7260.

[14] H. Haris, et al., Passively Q-switched Erbium-doped and ytterbium-doped fibre lasers with topological insulator bismuth selenide (Bi2Se3) as saturable absorber, Opt. Laser Technol. 88 (2017) 121–127.

[15] K. Park, et al., Black phosphorus saturable absorber for ultrafast mode-locked pulse laser via evanescent field interaction, Ann. Phys. 527 (11–12) (2015) 770–776.

[16] Q.L. Bao, et al., Atomic-layer graphene as a saturable absorber for ultrafast pulsed lasers, Adv. Funct. Mater. 19 (19) (2009) 3077–3083.

[17] Y.M. Chang, et al., Multilayered graphene efficiently formed by mechanical exfoliation for nonlinear saturable absorbers in fiber mode-locked lasers, Appl. Phys. Lett. 97 (21) (2010) 211102.

[18] U. Betz, et al., Thin films engineering of indium tin oxide: large area flat panel displays application, Surf. Coat. Technol. 200 (20–21) (2006) 5751–5759.

[19] X. Yan, et al., Refractive-index-matched indium–tin-oxide electrodes for liquid crystal displays, Japan. J. Appl. Phys. 48 (12R) (2009) 120203.

[20] L. Barraud, et al., Hydrogen-doped indium oxide/indium tin oxide bilayers for high-efficiency silicon heterojunction solar cells, Sol. Energy Mater. Sol. Cells 115 (2013) 151–156.

[21] H. Kim, et al., Electrical, optical, and structural properties of indium–tin–oxide thin films for organic light-emitting devices, J. Appl. Phys. 86 (11) (1999) 6451–6461.

[22] H. Kim, et al., Indium tin oxide thin films grown on flexible plastic substrates by pulsed-laser deposition for organic light-emitting diodes, Appl. Phys. Lett. 79 (3) (2001) 284–286.

[23] M.Z. Alam, I. De Leon, R.W. Boyd, Large optical nonlinearity of indium tin oxide in its epsilon-near-zero region, Science 352 (6287) (2016) 795–797.

[24] J. Guo, et al., Indium tin oxide nanocrystals as saturable absorbers for passively q-switched erbium-doped fiber laser, Opt. Mater. Express 7 (10) (2017) 3494–3502.

[25] L. Sun, et al., Preparation of few-layer bismuth selenide by liquid-phase-exfoliation and its optical absorption properties, Sci. Rep. 4 (1) (2014) 1–9.

[26] Z.Q. Luo, et al., 1-, 1.5-, and 2-mu m fiber lasers Q-switched by a broadband few-layer MoS2 saturable absorber, J. Lightwave Technol. 32 (24) (2014) 4077–4084.

[27] J. Sotor, et al., Mode-locking in Er-doped fiber laser based on mechanically exfoliated Sb 2 Te 3 saturable absorber, Opt. Mater. Express 4 (1) (2014) 1–6.

[28] Y. Chen, et al., Mechanically exfoliated black phosphorus as a new saturable absorber for both Q-switching and mode-locking laser operation, Opt. Express 23 (10) (2015) 12823–12833.

[29] B. Nizamani, et al., Indium tin oxide coated D-shape fiber as saturable absorber for passively Q-switched erbium-doped fiber laser, Opt. Laser Technol. 124 (2020) 105998.

[30] E.J. Aiub, et al., 200-fs mode-locked Erbium-doped fiber laser by using mechanically exfoliated MoS2 saturable absorber onto D-shaped optical fiber, Opt. Express 25 (9) (2017) 10546–10552.

[31] A.A.A. Jafry, et al., Q-switched ytterbium-doped fiber laser based on evanescent field interaction with lutetium oxide, Appl. Opt. 58 (35) (2019) 9670–9676.